FEBS Letters 580 (2006) 3018–3022

The structure of PknB in complex with mitoxantrone, an ATP-competitive inhibitor, suggests a mode of protein kinase regulation in mycobacteria

Annemarie Wehenkel[a,1], Pablo Fernandez[a,1], Marco Bellinzoni[a], Vincent Catherinot[b], Nathalie Barilone[c], Gilles Labesse[b], Mary Jackson[c], Pedro M. Alzari[a,*]

[a] *Unité de Biochimie Structurale and CNRS URA2185, Institut Pasteur, 25 rue du Docteur Roux, 75724 Paris, France*
[b] *Centre de Biochimie Structurale, INSERM U414, CNRS UMR5048, Université Montpellier 1, 15 Avenue Charles Flahault, 34060 Montpellier, France*
[c] *Unité de Génétique Mycobactérienne, Institut Pasteur, 25 rue du Docteur Roux, 75724 Paris, France*

Received 2 March 2006; revised 15 April 2006; accepted 18 April 2006

Available online 27 April 2006

Edited by Hans Eklund

Abstract ***Mycobacterium tuberculosis*** **PknB is an essential receptor-like protein kinase involved in cell growth control. Here, we demonstrate that mitoxantrone, an anthraquinone derivative used in cancer therapy, is a PknB inhibitor capable of preventing mycobacterial growth. The structure of the complex reveals that mitoxantrone partially occupies the adenine-binding pocket in PknB, providing a framework for the design of compounds with potential therapeutic applications. PknB crystallizes as a 'back-to-back' homodimer identical to those observed in other structures of PknB in complex with ATP analogs. This organization resembles that of the RNA-dependent protein kinase PKR, suggesting a mechanism for kinase activation in mycobacteria.**

Keywords: Drug design; Back-to-back dimerization; Crystal structure; Ser/Thr protein kinase-inhibitor complex; *Mycobacterium tuberculosis*

1. Introduction

The ability of *Mycobacterium tuberculosis*, the pathogen responsible for tuberculosis (TB), to adapt to changing environmental conditions requires an efficient way of sensing and transducing extracellular signals. One of the mechanisms used in mycobacteria to assure a tight regulation of cell growth and division involves the reversible phosphorylation on serine/threonine residues, a well-established process for eukaryotic signaling networks [1].

M. tuberculosis PknB is a trans-membrane Ser/Thr protein kinase (STPK) highly conserved in Gram-positive bacteria and apparently essential for mycobacterial viability [2]. The crystal structure of the kinase domain of PknB in complex with an ATP analogue [3,4] showed a striking conservation of both protein fold and catalytic mechanism between eukaryotic and prokaryotic STPKs. We have previously shown that PknB is regulated by autophosphorylation and dephosphorylation by the Ser/Thr protein phosphatase PstP [5,6] and recent work showed that PknB is predominantly expressed during exponential growth, where its overexpression causes morphological changes linked to defects in cell wall synthesis and cell division [7].

Aberrant kinase activity is implicated in numerous human diseases and, not surprisingly, protein kinases represent today one of the most important groups of drug targets [8,9]. Here we report that mitoxantrone, a compound used in cancer treatment, is a PknB inhibitor capable of preventing mycobacterial cell growth, suggesting that bacterial kinases may also represent a potential target for drug design. The crystal structure of the complex demonstrates that mitoxantrone is an ATP-competitive inhibitor of PknB and suggests a mode of regulation of protein kinases in mycobacteria.

2. Materials and methods

2.1. In silico screening

Over 40 000 compounds from different chemical libraries, including the Comprehensive Medicinal Chemistry database, were docked into the nucleotide-binding pocket of the *M. tuberculosis* PknB structure (pdb ID 1O6Y [3]) using the program FlexX [10].

2.2. Kinase assays

The kinase assays were carried out in 15 μl kinase buffer (50 mM HEPES, pH 7.0, 1 mM DTT, 0.01% Brij35, 5% glycerol, and 2 mM $MnCl_2$) using GarA as a substrate [6] (kinase:substrate molar ratio 1:2000). The reactions were started with the addition of 2.25 μM final ATP (containing 1 μCi of [γ-^{33}P]ATP), and carried out for 20 min at 30 °C. For the inhibition experiments, each compound was pre-incubated for 30 min at 4 °C with the reaction mixture (without ATP). The reactions were stopped by heat inactivation and the mixture transferred onto P81 paper (phosphocellulose, Whatman). The paper was washed with 1% phosphoric acid, rinsed with acetone and allowed to dry. Radiolabelled spots were analyzed with a PhosphorImager (Storm, Molecular Dynamics). IC_{50} values were determined using KaleidaGraph (Synergy Software).

2.3. Determination of MIC values

Minimal inhibitory concentration (MIC) values for mitoxantrone against different mycobacteria (Fig. 1c) were determined using the colorimetric resazurin microtiter assay in 7H9-OADC broth (Difco) at 37 °C, as described [11].

*Corresponding author. Fax: +33 145688604.
E-mail address: alzari@pasteur.fr (P.M. Alzari).

[1] These authors contributed equally to this work.

0014-5793/$32.00
doi:10.1016/j.febslet.2006.04.046

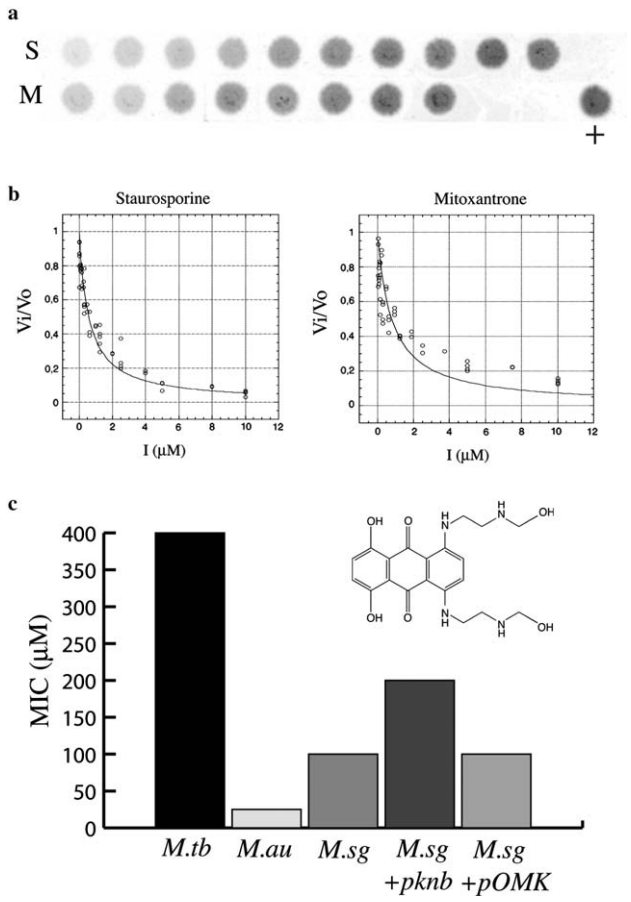

Fig. 1. Mitoxantrone inhibits PknB and prevents mycobacterial growth. (a) Radiolabelled spots of twofold serial dilutions of staurosporine (S; first spot: 10 μM) and mitoxantrone (M; first spot: 20 μM). A control without inhibitor (+) is included. (b) IC_{50} values for staurosporine and mitoxantrone. (c) Minimal inhibitory concentrations (MIC) values of mitoxantrone for different mycobacteria. (*M.tb*: *M. tuberculosis* H37Rv; *M.au*: *M. aurum* A+; *M.sg*: *M. smegmatis* mc^2155; *M.sg*+pknb: *M. smegmatis* mc^2155 overexpressing pknB; and *M.sg*+pOMK: *M. smegmatis* mc^2155 transformed with the control vector). Histogram values are representative of 2 or 3 independent experiments in each case. The chemical formula of mitoxantrone is shown in the inset.

2.4. Crystallography

The cytoplasmic domain of PknB (residues 1–279) was produced and purified as described [3]. Crystals of PknB (11 mg/ml) in complex with mitoxantrone (0.2 mM) (Sigma–Aldrich) appeared after 2 or 3 days in 1.2 M sodium acetate, 50 mM sodium cacodylate, pH 5.6, at 18 °C. After testing several crystals grown in slightly different conditions, we retained the best dataset from a single flash-frozen crystal collected on the ID14.3 beamline (ESRF, Grenoble) for further analysis (Table 1). The data are highly anisotropic (2.9 Å resolution limit along the c^* axis, but only 3.5 Å along the a^* and b^* axes), which accounts for the poor data completeness (data are 99% complete at 3.49 Å, 45% in the 3.49–3.21 Å shell, but only 16% in the 3.21–2.9 Å shell) and implies that the effective resolution may be around 3.2 Å. All crystallographic calculations were carried out using programs from the CCP4 software package [12]. Four independent monomers of PknB were positioned in the asymmetric unit by molecular replacement methods using the program PHASER [13] and the previously determined PknB structure (1O6Y) as a search probe. The bound ligand was clearly visible in the initial Fourier difference map for three out of the four independent monomers. After a few rounds of simulated annealing refinement using the program CNS [14] and manual model building with the program O [15], the crystallographic refinement was continued with the program REFMAC from CCP4 using tight non-crystallographic symmetry restraints and a translation/libration/screw model with eight different groups (corresponding to the N- and C-terminal lobes of each kinase domain in the asymmetric unit). The final parameters for the refined model are given in Table 1. Structure factors and atomic coordinates have been deposited with the Protein Data Bank (Accession Code 2FUM).

Table 1
Data collection and refinement statistics

Data collection	
Wavelength (Å)	0.931
Space group	$P4_32_12$
Cell dimensions [$a = b, c$] (Å)	116.9, 260.3
Unique reflections	28110
Resolution (Å)[a]	69.84–2.9 (2.97–2.9)
Multiplicity[a]	12.3 (2.6)
R_{meas}[a,b] refinement	0.12 (0.58)
Reflections used[c]	26678 (1432)
Resolution limits	70–2.9 Å
R-factor[d]	0.218
Free *R*-factor[d]	0.278
Number of refined atoms	
Protein	7890
Mitoxantrone	128
R.m.s. deviations	
Bond lengths (Å)	0.018
Bond angles (°)	1.901
Ramachandran outliers (%)	0.9

[a]Numbers in parentheses correspond to the highest resolution shell.
[b]$R_{meas} = \{\sum_h(\sqrt{\{n_h/n_h-1\}})\}\sum_j|\hat{I}_h - I_{h,j}|/\sum_{h,j}I_{h,j}$, where $\hat{I}_h = (\sum_j I_{h,j})/n_h$ and n_h is the multiplicity of reflection h.
[c]The number of reflections used for free *R*-factor calculation is shown in parentheses.
[d]*R*-factor $= \sum_{hkl}||F_o| - k|F_c||/\sum_{hkl}|F_o|$.

2.5. Sequence and structural comparisons

A homology search using the PknB sequence against all finished bacterial genomes (NCBI, as of December 2005) identified 39 trans-membrane kinases with predicted extracellular PASTA domains. The sequences were aligned and the residue conservation pattern was mapped onto the structure (Fig. 3b) using the program ConSurf [16].

3. Results and discussion

3.1. Mitoxantrone inhibits mycobacterial growth in culture

We carried out an *in silico* screening to search for PknB inhibitors (see Section 2), and 20 commercially available compounds from the first 60 hits were then tested for their inhibitory properties. Kinase assays revealed that mitoxantrone (1,4-dihydroxy-5,8-bis[2-(hydroxyethylamino)-ethylamino]-9,10-anthracenedione) was able to inhibit PknB with an IC_{50} in the micromolar range ($IC_{50} = 0.8 \pm 0.05$ μM), comparable to that observed for the cytotoxic large-spectrum kinase inhibitor staurosporine ($IC_{50} = 0.6 \pm 0.05$ μM), see Fig. 1a/b. Mitoxantrone is a DNA-reactive agent that has been used for several years in cancer treatment [17]. Besides its DNA-binding properties, other mechanisms to account for mitoxantrone cytotoxicity may involve free radical production [18] and inhibition of Ser/Thr protein kinases [19,20].

Mitoxantrone showed an inhibitory effect on cell growth (Fig. 1c) when tested on cultures of *M. tuberculosis* (MIC = 400 μM), *M. smegmatis* mc^2155 (MIC = 100 μM), and *M. aurum* A+ (MIC = 25 μM) using the resazurin microtiter assay. Differences in the permeability of the cell envelope and/or in the structure of the targets of mitoxantrone in the

three mycobacterial species may account for the different MICs observed. The effect of mitoxantrone on *M. smegmatis* was partially reversed when the wild-type strain was transformed with a multicopy replicative plasmid (pOMK) [21] carrying a wild-type copy of the *M. tuberculosis pknB* gene expressed from its own promoter. The MIC of the *pknB* overexpressor was twofold those of the wild-type strain (200 μM) or the strain transformed with the control vector alone (Fig. 1c), suggesting that PknB is at least one of the lethal targets of mitoxantrone in this species.

3.2. Structure of the PknB-inhibitor complex

To investigate the mode of action of mitoxantrone on PknB, we crystallized the complex and determined its 3D structure by X-ray diffraction methods (Table 1). The overall structure of the enzyme is similar to those previously described for PknB in complex with ATP analogs [3,4], with the kinase domain in an overall closed conformation and a disordered activation loop. The most noticeable structural change involves the glycine-rich loop, which in the absence of ATP moves further towards the C-terminal lobe (Fig. 2a).

Clear electron density is observed for mitoxantrone in the nucleotide-binding cleft of PknB (Fig. 2b). The planar dihydroxy anthraquinone moiety of the inhibitor occupies the hydrophobic cage that binds the adenosine moiety of ATP. An important number of residues of both the N- and C-terminal lobes makes van der Waals contacts with the inhibitor, including Leu17, Gly18, Val25, Ala38, Met 92, Glu93, Tyr94 and Val95 in the N-terminal lobe, Met145 and Met155 in the C-terminal lobe. The main-chain amide group of Val95, which in the PknB-AMPPCP complex is hydrogen bonded to the N1 atom of adenosine [3], now forms a hydrogen bonding interaction with one hydroxyl group of the inhibitor (Fig. 2c). This interaction may account for the observed lateral positioning of the inhibitor within the wide hydrophobic binding pocket (Fig. 2b). The partial occupancy of the cleft leaves space to accommodate bulkier substituents at the three-ring moiety, which might be exploited to improve the inhibitory properties of the compound.

The limited resolution of this study precludes a detailed analysis of the interactions made by the flexible hydroxyethylamino moieties of the ligand, although in at least two of the four independent PknB molecules the side-chain of Asn143 makes additional hydrogen bonding interactions with the nitrogen atom of one hydroxyethylamino moiety. As observed in other protein kinase-inhibitor complexes [9], it is possible that these flexible extended moieties, which protrude away from the ATP-binding pocket, could interfere with the active conformation of the kinase and account in part for the inhibitory properties of mitoxantrone.

3.3. The conserved dimeric arrangement of PknB is similar to that of PKR

When expressed as a recombinant protein, the catalytic domain of PknB was observed to behave as a mixture of monomers and dimers in solution (Ref. [4] and data not shown). Interestingly, in the PknB-mitoxantrone complex the kinase domain crystallized as a 'back-to-back' homodimer (Fig. 3a). The two crystallographically independent dimers in the complex are very similar to each other and to those observed in two other structures of PknB crystallized in different space

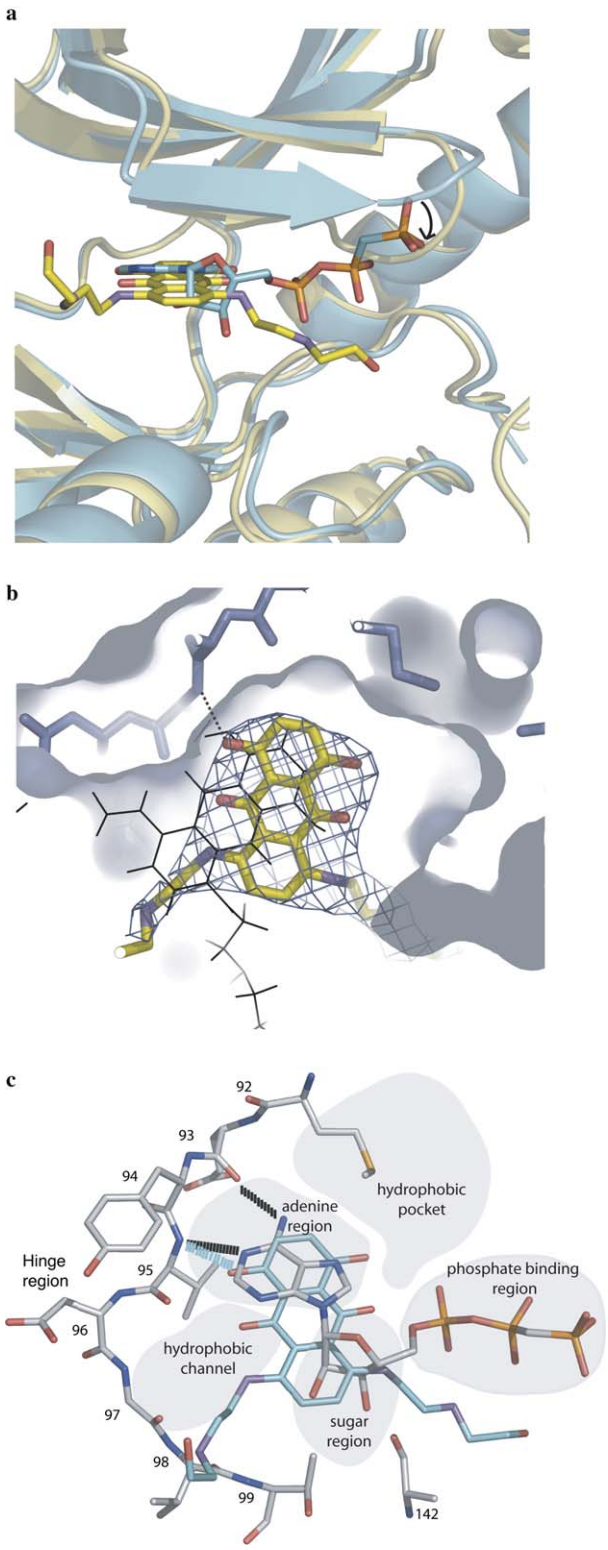

Fig. 2. Structure of the PknB-mitoxantrone complex. (a) Superposition of the PknB-mitoxantrone complex (in yellow) and the PknB-AMPPCP complex (1O6Y, in cyan). Note the movement of the Gly-rich loop (black arrow). (b) Observed (yellow) and predicted (thin lines) orientations of mitoxantrone within the adenosine-binding cavity (represented as a molecular surface). The electron density map for the inhibitor is contoured at 1σ. (c) Schematic view (represented as in Ref. [26]) of the PknB ATP-binding site showing hydrogen bonding interactions with both the inhibitor (in blue) and AMP-PCP (PDB code 1O6Y).

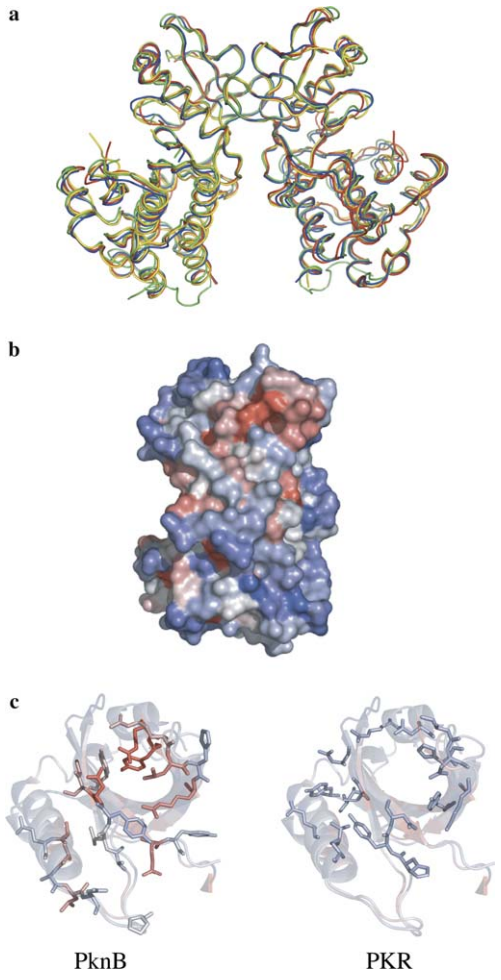

Fig. 3. The conserved PknB homodimer. (a) Superposition of the two crystallographically independent homodimers from the PknB-mitoxantrone complex (in red and green) with those observed in the PknB-nucleotide complexes 1O6Y [3] (in blue) and 1MRU [4] (in yellow). (b) Overall view of the PknB monomer (rotated 90° along the vertical axis with respect to the right monomer in Fig. 3a), color-coded according to amino acid conservation (red: highly conserved) in 39 PknB-like protein sequences from 35 different bacterial species (*Bacillus anthracis*, *B. cereus*, *B. clausii*, *B. licheniformis*, *B. subtilis*, *Bifidobacterium longum*, *Clostridium acetobutylicum*, *C. perfringens*, *C. tetani*, *Corynebacterium diphtheriae*, *C. efficiens*, *C. glutamicum*, *Enterococcus faecalis*, *Geobacillus kaustophilus*, *Lactobacillus acidophilus*, *L. johnsonii*, *Listeria monocytogenes*, *Mycobacterium avium*, *M. bovis*, *M. leprae*, *M. tuberculosis*, *Nocardia farcinica*, *Nocardioides*, *Leifsonia xyli*, *Oceanobacillus iheyensis*, *Propionibacterium acnes*, *Staphylococcus haemolyticus*, *S. saprophyticus*, *Streptococcus agalactiae*, *S. mutans*, *S. pyogenes*, *Streptomyces coelicolor*, *Symbiobacterium thermophilum*, *Thermoanaerobacter tengcongensis*, *Thermobifida fusca*). (c) Comparison of the PknB and RNA-dependent PKR dimer interfaces. The side-chain residues belonging to the interfaces are shown (PknB color-coded as in (b)).

groups [3,4], lending strong support to the hypothesis that this homodimeric arrangement is physiologically relevant [4].

The dimer interface, composed almost exclusively of residues from the N-lobe, is largely conserved in PknB-like bacterial protein kinases (Fig. 3b). When the amino acid sequences of 39 *pknB* putative ortholog genes are mapped onto the PknB structure, 8 positions at the dimer interface are almost invariably conserved (i.e. conserved in at least 35 of the 39 protein sequences): Arg10, Leu33, Arg35, Ala60, Pro69, Asp76, Gly78 and Glu93. The strictly invariant residues Arg10 and Asp76 form a double intermolecular salt bridge in the homodimer. Two other highly conserved residues are also engaged in intermolecular hydrogen-bonding interactions: the guanidium group of Arg35 forms two hydrogen bonds with the main-chain oxygen atoms of residues Ala64 and Val74, and the side-chain of Asn67 forms a hydrogen bond with the carboxylate group of Glu93. Interestingly, the main-chain atoms of Glu93 are hydrogen-bonded to the ATP analog in the binary complex (and are also in contact with mitoxantrone in the PknB-inhibitor complex), thus establishing a direct link between the dimer interface and the nucleotide-binding site.

Remarkably, the PknB homodimer strongly resembles that recently observed for the RNA-dependent antiviral protein kinase PKR [22] (Fig. 3c). In both cases the same equivalent positions are involved in the interface and a similar surface area is occluded upon dimer formation: the PknB interface is made up of 23 residues (80 atoms) that contribute 800 $Å^2$ to the contact surface area, while the PKR dimer interface includes 26 residues (78 atoms) and has a buried surface area of 730 $Å^2$ per monomer. Whereas a precise understanding of how PknB dimerization can directly influence the catalytic activity must await the structural study of the enzyme in a repressed monomeric state, the striking similarity between the PknB and PKR homodimers allows us to speculate on a possible role of dimerization on PknB activity regulation, based on the analogy with PKR [22,23]. Thus, in its monomeric state, PknB would be inactive due, for instance, to a misplacement of helix αC (whose C-terminal end is within the dimer interface), in much the same way as proposed for other eukaryotic protein kinases. Upon ligand binding, the extracellular region would then promote 'back-to-back' dimerization of the catalytic domain, as observed in the crystal structure. Indeed, the influence of the extracellular domain on dimerization was demonstrated for the PknB-like protein kinase PrkC from *B. subtilis* [24]. In turn, PknB homodimer formation would then promote autophosphorylation at Ser/Thr residues in the activation loop [5,25] and subsequent substrate recruitment [6,7].

While many aspects of the above model remain necessarily speculative at this stage, it suggests a possible strategy for drug design based on ATP-competitive lead compounds such as mitoxantrone derivatives. Given the direct structural links between PknB dimerization, catalytic activity and nucleotide binding, it should be possible to obtain specific ATP-competitive inhibitors that either block the catalytic domain in an inactive state or just preclude 'back-to-back' dimerization.

Acknowledgements: The authors thank Martin Graña for helpful discussions. This work has been supported by grants from the Institut Pasteur (GPH-Tuberculose) and the European Commission (X-TB, contract QLK2-CT-2001-02018).

References

[1] Hunter, T. (2000) Signaling-2000 and beyond. Cell 100, 113–127.
[2] Sassetti, C.M., Boyd, D.H. and Rubin, E.J. (2003) Genes required for mycobacterial growth defined by high density mutagenesis. Mol. Microbiol. 48, 77–84.
[3] Ortiz-Lombardia, M., Pompeo, F., Boitel, B. and Alzari, P.M. (2003) Crystal structure of the catalytic domain of the PknB serine/threonine kinase from *Mycobacterium tuberculosis*. J. Biol. Chem. 278, 13094–13100.
[4] Young, T.A., Delagoutte, B., Endrizzi, J.A., Falick, A.M. and Alber, T. (2003) Structure of *Mycobaterium tuberculosis* PknB

supports a universal activation mechanism for Ser/Thr protein kinases. Nat. Struct. Biol. 10, 168–174.
[5] Boitel, B., Ortiz-Lombardia, M., Duran, R., Pompeo, F., Cole, S.T., Cerveñansky, C. and Alzari, P.M. (2003) PknB kinase activity is regulated by phosphorylation in two Thr residues and dephosphorylation by PstP, the cognate phospho-Ser/Thr phosphatase, in *Mycobacterium tuberculosis*. Mol. Microbiol. 49, 1493–1508.
[6] Villarino, A., Duran, R., Wehenkel, A., Fernandez, P., England, P., Brodin, P., Cole, S.T., Zimny-Arndt, U., Jungblut, P.R., Cerveñansky, C. and Alzari, P.M. (2005) Proteomic identification of *M. tuberculosis* protein kinase substrates: PknB recruits GarA, a FHA-containing protein, through activation loop-mediated interactions. J. Mol. Biol. 350, 953–963.
[7] Kang, C.M., Abbott, D.W., Park, S.T., Dascher, C.C., Cantley, L.C. and Husson, R.N. (2005) The *Mycobacterium tuberculosis* serine/threonine kinases PknA and PknB: substrate identification and regulation of cell shape. Genes Dev. 19, 1692–1704.
[8] Cohen, P. (2002) Protein kinases, the major drug targets of the 21st century? Nat. Rev. Drug Discov. 1, 309–316.
[9] Noble, M.E.M., Endicott, J.A. and Johnson, L.N. (2004) Protein kinase inhibitors: insights into drug design from structure. Science 303, 1800–1805.
[10] Rarey, M., Wefing, S. and Lengauer, T. (1996) Placement of medium-sized molecular fragments into active sites of proteins. J. Comp. Aided Mol Des. 10, 41–54.
[11] Martin, A., Camacho, M., Portaels, F. and Palomino, J.-C. (2003) Resazurin microtiter assay plate testing of *Mycobacterium tuberculosis* susceptibilities to second-line drugs: rapid, simple, and inexpensive method. Antimicrob. Agents Chemotherap. 47, 3616–3619.
[12] CCP4, Collaborative Computational Project Number (1994) Acta Cryst. D 50, 760–763.
[13] McCoy, A.J., Grosse-Kunstleve, R.W., Storoni, L.C. and Read, R.J. (2005) Likelihood-enhanced fast translation functions. Acta Cryst. D 61, 458–464.
[14] Brunger, A.T., Adams, P.D., Clore, G.M., Gros, P., Grosse-Kunstleve, R.W., Jiang, J-S., Kuszewski, J., Nilges, M., Pannu, N.S., Read, R.J., Rice, L.M., Simonson, T. and Warren, G.L. (1998) Crystallography & NMR system (CNS): a new software system for macromolecular structure determination. Acta Cryst. D 54, 905–921.
[15] Jones, T.A., Zhou, J.Y., Cowan, S.W. and Kjeldgaard, M. (1991) Improved methods for building protein models in electron density maps and the location of errors in these models. Acta Cryst. A 47, 110–119.
[16] Glaser, F., Pupko, T., Paz, I., Bell, R.E., Bechor-Shental, D., Martz, E. and Ben-Tal, N. (2003) ConSurf: identification of functional regions in proteins by surface-mapping of phylogenetic information. Bioinformatics 19, 163–164.
[17] Shenkenberg, T.D and Von Hoff, D.D. (1986) Mitoxantrone: a new anticancer drug with significant clinical activity. Ann. Int. Med. 105, 67–81.
[18] Basra, J., Wolf, C.R., Brown, J.R. and Patterson, L.H. (1985) Evidence for human liver mediated free-radical formation by doxorubicin and mitoxantrone. Anticancer Drug Des. 1, 45.
[19] Jinsart, W., Ternai, B. and Polya, G.M. (1992) Inhibition of myosin light chain kinase, cAMP-dependent protein kinase, protein kinase C and of plant Ca(2+)-dependent protein kinase by anthraquinones. Biol. Chem. Hoppe-Seyler 373, 903–910.
[20] Takeuchi, N., Nakamura, T., Takeuchi, F., Hashimoto, E. and Yamamura, H. (1992) Inhibitory effect of mitoxantrone on activity of protein kinase C and growth of HL60 cells. J. Biochem. (Tokyo) 112, 762–767.
[21] Jackson, M., Berthet, F.-X., Otal, I., Rauzier, J., Martin, C., Gicquel, B. and Guilhot, C. (1996) The *Mycobacterium tuberculosis* purine biosynthetic pathway: isolation and characterization of the *purC* and *purL* genes. Microbiology 142, 2439–2447.
[22] Dar, A.C., Dever, T.E. and Sicheri, F. (2005) Higher-order substrate recognition of eIF2a by the RNA-dependent protein kinase PKR. Cell 122, 887–900.
[23] Dey, M., Cao, C., Dar, A.C., Tamura, T., Ozato, K., Sicheri, F. and Dever, T.E. (2005) Mechanistic link between PKR dimerization, autophosphorylation and eIF2a substrate recognition. Cell 122, 901–913.
[24] Madec, E., Laszkiewicz, A., Iwanicki, A., Obuchowski, M. and Seror, S. (2002) Characterization of a membrane-linked Ser/Thr protein kinase in *Bacillus subtilis*, implicated in developmental processes. Mol. Microbiol. 2, 571–586.
[25] Duran, R., Villarino, A., Bellinzoni, M., Wehenkel, A., Fernandez, P., Boitel, B., Cole, S.T., Alzari, P.M. and Cervenansky, C. (2005) Conserved autophosphorylation pattern in activation loops and juxtamembrane regions of *M. tuberculosis* Ser/Thr protein kinases. Biophys. Biochem. Res. Commun. 333, 858–867.
[26] Traxler, P. and Furet, P. (1999) Strategies toward the design of novel and selective protein tyrosine kinase inhibitors. Pharmacol. Ther. 82, 195–206.